

**Mixed Lineage Kinase 3 (MLK3) functions as a cGMP-
dependent protein kinase I alpha (PKGI α) substrate
and inhibits cardiac remodeling *in vivo***

A thesis

Submitted by

Robert M. Blanton, Jr

In partial fulfillment of the requirements
for the degree of

Master of Science

in

Clinical and Translational Science

TUFTS UNIVERSITY

Sackler School of Biomedical Sciences

February, 2017

Advisors:

Thesis Chair: Gordon S. Huggins MD

Project Mentor: Richard H. Karas MD, PhD

Statistical Mentor: Farzad Noubary, PhD

Abstract

Protein kinase G I (PKGI) prevents cardiac hypertrophy and dysfunction in the failing heart. Although PKGI-activating drugs remain under investigation for the treatment of heart failure, the downstream molecular substrates through which PKGI regulates these processes remain incompletely understood. In this study we identified one candidate PKGI α substrate in the myocardium, Mixed Lineage Kinase 3, (MLK3) an upstream regulator of stress-responsive JNK signaling. We first tested for a PKGI α -MLK3 protein-protein interaction with endogenous proteins in the myocardium by co-immunoprecipitation. We confirmed direct PKGI α -MLK3 interaction with affinity purified proteins. In cultured cardiac myocytes MLK3 mediated cGMP-stimulated JNK phosphorylation, and pharmacologic inhibition of MLK3 kinase activity induced cardiomyocyte hypertrophy. MLK3 protein expression increased in myocardial tissues from humans with end-stage heart failure and cardiac remodeling. Mice with genetic deletion of MLK3 (MLK3^{-/-}) exhibited baseline cardiac hypertrophy with preserved cardiac function and structure. In response to pressure overload, MLK3^{-/-} mice had worsened cardiac function and increased cardiomyocyte hypertrophy. Together these data demonstrate MLK3 is a novel PKGI α substrate, indicate MLK3 functions as a cardioprotective molecule, and further support the approach of exploring myocardial PKGI α -substrates to identify novel anti-remodeling molecules.

Acknowledgements

Thesis Committee: Gordon S. Huggins MD Chair
 Farzad Noubary PhD Statistical Mentor
 Richard H. Karas MD, PhD

Educational mentors: David Kent MD, MSc
 Jessica Paulus ScD
 Farzad Noubary PhD
 Norma Terrin PhD
 Angie Mae Rodday PhD
 Robert J. Goldberg PhD

The Molecular Cardiology Research Institute, and the Division of Cardiology at Tufts Medical Center

Wanda, Lauren, and Robert (Robby) Blanton for their patience and support.

Table of Contents

Abstract	i
Acknowledgements	ii
Table of Contents	iii
List of Tables	v
List of Figures	vi
List of Abbreviations	vii
Introduction	1
1.1 Pathologic cardiac remodeling.....	1
1.2 cGMP-dependent Protein Kinase G as an antiremodeling molecule.....	3
1.3 Rationale for identifying cardiac PKGI α substrates.....	6
1.4 Central hypothesis.....	8
Materials and Methods	9
2.1 Regulatory approval.....	9
2.2 Cell culture.....	9
2.3 cDNA Expression Plasmids.....	9
2.4 Protein-protein interaction studies.....	10
2.5 GST fragment interaction studies in mouse LV lysates.....	10
2.6 Native immunoprecipitation of MLK3 from mouse LV lysates.....	11
2.7 Western blotting.....	11
2.8 PKGI α target phosphorylation site prediction.....	11
2.9 Kinase reactions.....	12
2.10 Cell Culture Studies.....	12
2.11 Adult mouse cardiomyocyte (AMCM) culture.....	12
2.12 Adult rat ventricular myocyte (ARVM) culture.....	13
2.13 Experimental animals.....	13
2.14 Transthoracic echocardiography.....	13
2.15 Transaortic constriction.....	14
2.16 LV in vivo hemodynamic measurements.....	14
2.17 Histological analysis.....	14
2.18 qRT-PCR analysis.....	14
2.19 Human heart samples.....	15
2.20 Statistical Methods.....	15
2.21 Statistical analysis of protein expression from human heart samples.....	16
Results	16
3.1 PKGI and MLK3 co-interact in the LV.....	16
3.2 PKGI α induction of MLK3 phosphorylation.....	17
3.3 Inhibition of MLK3 kinase activity represses JNK activation in the cardiac.....	21
myocyte and promotes cardiac myocyte hypertrophy.	
3.4 MLK3 expression increases in the pressure overloaded LV, and in the failing...21	
human LV.	
3.5 MLK3 deletion leads to increased LV dysfunction and hypertrophy after pressure	
overload.....	24
Discussion	28

4.1 Leucine zipper dependent binding of PKGI α and MLK3.....	28
4.2 Regulation of MLK3 expression in the failing LV.....	30
4.3 MLK3 promotes JNK phosphorylation and inhibits CM hypertrophy.....	31
4.4 Role of MLK3 in the LV response to pressure overload in vivo.....	32
4.5 Clinical relevance of MLK3 as novel regulator of cardiac remodeling.....	33
4.6 Significance of MLK3 as a PKGI α LZ-dependent substrate.....	35
4.7 Limitations.....	36
4.8 Conclusions.....	36
References.....	37

List of Tables

Table 1: Baseline data in MLK3 ^{+/+} and MLK3 ^{-/-} mice.....	25
---	----

List of Figures

Figure 1: Summary of PKGI activation pathway in cardiovascular tissues.....	4
Figure 2: PKGI α interacts with MLK3 in LZ-dependent manner.....	18
Figure 3: PKGI α stimulates MLK3 phosphorylation on the activation loop residues Thr-277 / Ser-281.....	19
Figure 4: MLK3 required for cGMP-induced JNK phosphorylation in cardiomyocytes..	20
Figure 5: Inhibition of MLK3 kinase activity blocks JNK activation in the cardiac myocyte and causes cardiac myocyte hypertrophy.....	22
Figure 6: MLK3 expression is increased in the left ventricle after pressure overload, and in the human failing left ventricle.....	23
Figure 7. MLK3 ^{-/-} mice develop increased cardiac dysfunction after pressure overload..	26
Figure 8. MLK3 ^{-/-} mice develop increased pathologic LV hypertrophy and fibrotic gene expression after pressure overload.....	27

List of Abbreviations

ARVM	Adult rat ventricular myocytes
CDC42	Cell division control protein 42
cGMP	Cyclic guanosine monophosphate
CM	Cardiac myocyte
dP/dt _{max}	Maximum rate of left ventricular pressure rise
dP/dt _{min}	Maximum rate of left ventricular pressure decline
FS	Left ventricular fractional shortening percentage
GST	Glutathione S-transferase
HCM	Hypertrophic cardiomyopathy
JNK	c-Jun N-terminal kinase
LV	Left ventricle
LZ	Leucine zipper
MEKK1	Mitogen activated protein kinase/Extracellular recognition kinase kinase 1
MKK	Mitogen activated protein kinase kinase
MLK3	Mixed lineage kinase 3
NDRI	National disease research interchange
NICM	Nonischemic cardiomyopathy
NO	Nitric oxide
NP	Natriuretic peptide
PKGI α	cGMP-dependent protein kinase I alpha
Ser	Serine
TAC	Transaortic constriction
Thr	Threonine
WT	Wild type

Introduction

Heart failure represents a major cause of mortality and remains the most common cause of hospitalization in the US¹. The clinical syndrome of heart failure includes symptoms such as shortness of breath, lower extremity edema, and fatigue. These symptoms occur predominantly from the inability of the heart to provide sufficient cardiac output to meet the metabolic demands of the body². For example, reduced cardiac output and resultant low blood pressure contributes to generalized fatigue and exercise intolerance. Additionally, in many cases, cardiac output remains normal, but this comes at the expense of requiring higher ventricular filling pressures to generate the cardiac output, which leads to elevation of left atrial pressure and causes back pressure into the lungs and right sided circulation. These hemodynamic changes are thought to produce the symptoms of dyspnea (from pulmonary edema) and fluid retention (from right sided pressure overload and edema) which mark the heart failure syndrome.

1.1 Pathologic Cardiac Remodeling

This syndrome of heart failure arises from the process of pathologic cardiac remodeling, defined as the structural and functional abnormalities that occur in the heart in response to pathologic stress². In humans these pathologic stresses include myocardial infarction, pressure overload (such as hypertension or aortic stenosis), and genetic mutations. At the organ level, cardiac remodeling is marked initially by increased cardiac size (defined as cardiac hypertrophy), with preserved systolic pumping function. Over time, this phenotype typically progresses to one of reduced systolic function and chamber dilation, leading to the symptoms and mortality described above.

At the cellular level, cardiac remodeling is marked by dysfunction of the cardiac myocyte, the principle contractile cell of the heart, as well as increased cardiac myocyte death (apoptosis), and interstitial fibrosis^{2,3}. Further, the remodeled heart reverts to a pattern known as fetal gene expression, in which genes typically expressed during only fetal heart development become re-expressed in the adult heart. For example, in the remodeled left ventricle (LV), the fetal beta isoform of myosin heavy chain replaces the normal adult, or alpha, isoform. Further, whereas the normal adult heart derives most of its energy from oxidation of fatty acids, the remodeled and failing heart reverts to the fetal pattern of primarily metabolizing glucose³.

Multiple basic and translational studies over the last several decades have established that this process of stress-induced cardiac hypertrophy and remodeling is maladaptive rather than compensatory. In other words, drawing from scientific studies, the current paradigm holds that cardiac remodeling actually promotes the development of heart failure, and conversely attenuating the cardiac remodeling response can ameliorate or even prevent heart failure. These experimental studies have been corroborated by observational studies demonstrating that pharmacologic therapies which improve outcomes in patients with heart failure also attenuate or even improve adverse cardiac remodeling⁴.

Therefore, improved understanding of the pathophysiologic mechanisms promoting cardiac remodeling holds the potential to produce improved therapies for heart failure. The cardiac remodeling process is highly regulated by intracellular molecular signaling pathways. For example, in response to pathologic stimuli, some pro-remodeling signaling cascades become up-regulated leading over time to progressive ventricular

dysfunction and clinical heart failure. Conversely, cardioprotective signaling pathways which slow down or inhibit this process often become downregulated or even inhibited. However, the complete signaling mechanisms which regulate cardiac remodeling remain unknown, and in particular those pathways which oppose the remodeling process are incompletely understood.

1.2 cGMP-dependent Protein Kinase G as an antiremodeling molecule.

In the present study we have therefore investigated the mechanisms through which the signaling molecule known as cGMP-dependent protein kinase I alpha (PKGI α) attenuates cardiac remodeling. PKGI α is a kinase, meaning that it is an enzyme that interacts with other specific substrate molecules and covalently adds a phosphate on specific amino acids. Phosphorylation of target proteins can alter protein structure, function, or localization and therefore represents a basic signaling mechanism through which cells can rapidly adapt to extracellular signals. PKGI α is itself directly activated by the intracellular second messenger molecule cyclic GMP (cGMP). As outlined in Figure 1, in the cardiovascular system, cGMP is generated by enzymes called guanylate cyclases (reviewed in 5). Guanylate cyclases can be activated by natriuretic peptides which act on the cell membrane-associated form of guanylate cyclase, or by nitric oxide which diffuses across cell membranes to activate the soluble, cytosolic form of guanylate cyclase. In summary, these pathways allow cells to tightly regulate PKGI α kinase activity by generating cGMP through exposure to natriuretic peptides or NO.

The cardiovascular function of PKGI α has been best studied in blood vessels. Specifically, in the vascular smooth muscle cell, NO or NPs increase cGMP to activate PKGI α kinase activity, which promotes vascular smooth muscle relaxation, leading to

vasodilation of resistance arterioles and subsequent reduction of blood pressure⁵. Over the past two decades, many of the precise vasodilating substrates that PKGI α binds and

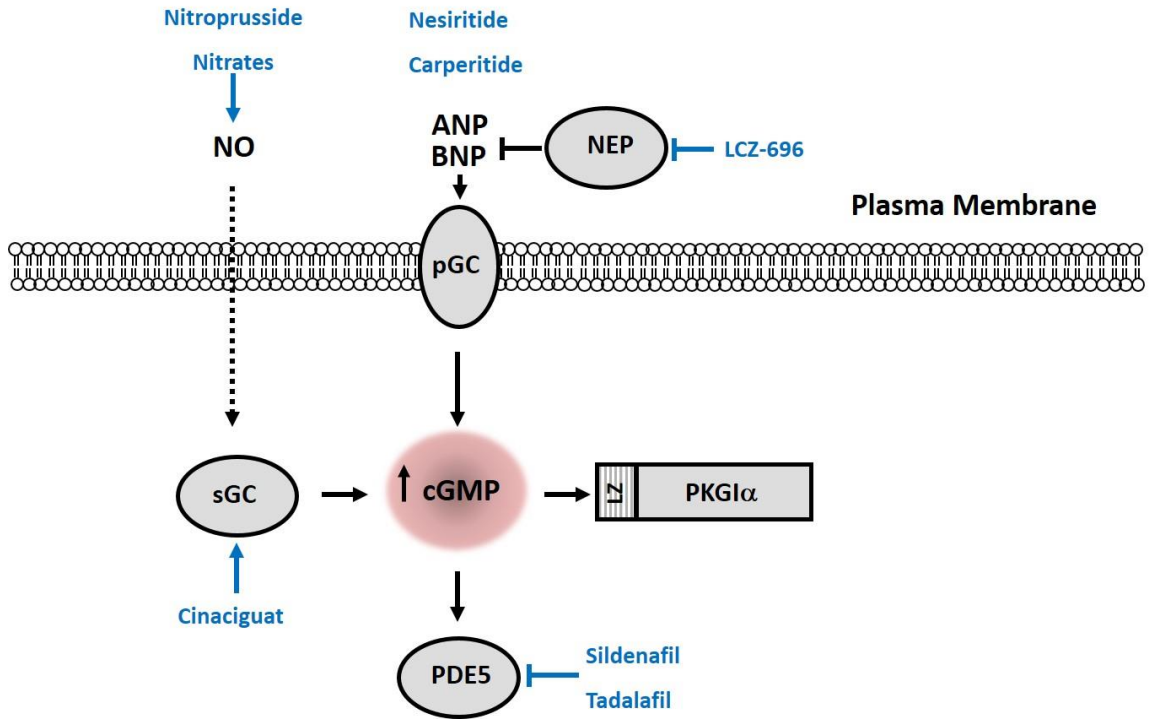


Figure 1. Summary of PKGI activation pathway in cardiovascular tissues. Currently available pharmacologic agents targeting specific components of the pathway are shown in blue. Also represented are the hypothesized overlapping, but non-identical, protein kinase G I (PKGI α) substrates in the vascular smooth muscle cell and cardiac myocyte, which may mediate vasodilation and attenuation of cardiac remodeling, respectively. NO indicates nitric oxide, ANP, atrial natriuretic peptide; BNP, B-type natriuretic peptide; LZ, leucine zipper domain; NEP, neutral endopeptidase (neprilysin); pGC, particulate guanylate cyclase (NP receptor); and sGC, soluble guanylate cyclase.

phosphorylates in vascular smooth muscle cells have been identified, and this has led to an improved understanding of the biology of blood pressure regulation and hypertension.

In contrast to the blood vessel, the role of PKGI α in the heart and particular in the cardiac myocyte has been less completely studied. Specifically, the precise substrates that PKGI α binds and phosphorylates in the heart remain unknown. However, several factors highlight the need to better understanding the biology of PKGI α in heart failure. First, multiple preclinical studies support that upstream PKGI α activators like NO, natriuretic peptides, and cGMP inhibit cardiac remodeling, both in cell culture and in animal experimental models of heart failure⁵. Second, in addition to these pre-clinical studies, multiple PKGI activating drugs remain under active investigation for the treatment of heart failure. For example, the recent PARADIGM-HF trial demonstrated that inhibition of the molecule neprilysin with the drug LCZ696, when added to standard therapy, improves outcomes in patients with heart failure and reduced ejection fraction⁶. Neprilysin is an enzyme which degrades natriuretic peptides^{5,6}. Therefore, inhibiting neprilysin preserves natriuretic peptide availability and indirectly promotes PKGI α kinase activity. Further, treatment with nitric oxide donors has been shown to improve heart failure outcomes when combined with the vasodilator hydralazine⁵. These clinical studies support the translational importance of understanding the biological mechanisms through which activators of PKGI α lead to improved outcomes in heart failure. These mechanisms, however, remain poorly understood.

Moreover, despite the aforementioned successes of PKGI-activating drugs for the treatment of chronic heart failure, a number of studies of these drugs have either failed to improve outcomes, or in some cases have been terminated early due to excessive side effects like hypotension⁵. Even the PARADIGM-HF trial described above reported much higher rates of symptomatic hypotension in patients receiving LCZ696 compared with

control-treated patients⁶. The excess hypotension observed with PKG activating drugs likely arises from vasodilation resulting from PKGI induction of vascular smooth muscle cell relaxation.

It would be an attractive therapeutic strategy, therefore, to find therapies which promote PKGI α anti-remodeling mechanisms in the heart, but avoid PKGI α -induced vasodilation. One way to do this would be to treat patients with therapies which selectively activate PKGI only in the heart or cardiac myocyte but not in the vasculature. While such tissue-selective strategies are in fact feasible in animals⁷ and in some cases have been trialed in humans, they remain investigational therapies. An alternative approach would be to identify PKGI α substrates which regulate cardiac remodeling but do not severely affect blood pressure. For example, we recently demonstrated that PKGI α phosphorylates a protein termed cardiac myosin binding protein-C, and that it phosphorylates this protein in such a way that inhibits cardiac remodeling⁸. Cardiac myosin binding protein C is expressed selectively in cardiac myocytes, not vascular tissues, which supports the concept that PKGI α substrates do exist that selectively inhibit cardiac remodeling but do not affect blood pressure.

1.3 Rationale for identifying cardiac PKGI α substrates.

In the current study, we aimed to identify additional new PKGI α substrates. Moreover, we wanted to identify PKGI α substrates which had not previously been implicated in cardiovascular biology. As such, our scientific goals were three-fold. First, by exploring the downstream substrates of PKGI α in the heart we hope to uncover new biologic mechanisms that regulate cardiac structure and function. Understanding these basic mechanisms could further scientific knowledge and improve our understanding of

cardiac biology and pathophysiology in general. Second, from a translational perspective, we hypothesize that identifying PKGI α substrates which inhibit cardiac remodeling might actually reveal new candidate therapeutic targets for the treatment of heart failure. Third, from more practical perspective, focusing on PKGI α substrates in the heart, as opposed to the blood vessel, might eventually identify selective strategies to inhibit cardiac remodeling yet avoid excessive hypotension arising from systemic PKGI α activation.

PKGI α contains a region termed the leucine zipper (LZ) domain⁹. This domain is located at the N-terminal portion of the protein and contains multiple leucine residues. Because leucine is a hydrophobic amino acid, the LZ domain is also highly hydrophobic and this targets PKGI α to portions of proteins which contain their own hydrophobic domains. Often, LZ domains intercalate tightly with LZ domains on other proteins which gives rise to the “zipper” terminology^{9,10}. Thus, the LZ domain helps direct PKGI α to specific kinase substrates within the cell. Our previous investigations have revealed that PKGI α inhibition of cardiac remodeling requires an intact PKGI α leucine zipper (LZ) domain¹¹. The LZ domain mediates PKGI α binding to key effectors in the cardiovascular system⁹. In mice, an inactivating mutation of the LZ domain leads to increased LV hypertrophy, remodeling, and systolic and diastolic dysfunction after pressure overload, as well as markedly accelerated mortality¹¹, supporting a critical role of the PKGI α LZ domain in attenuating cardiac remodeling.

Although the PKGI α LZ domain is required for attenuation of pathologic cardiac remodeling and heart failure, the specific LZ-binding proteins mediating the inhibition of remodeling have not been identified. Prior studies have identified that the PKGI α LZ

domain mediates activation of a signaling molecule termed c-Jun n-terminal kinase, (JNK), as early as 48 hours after pressure overload¹¹. JNK activation normally preserves LV systolic function after pressure overload¹², and JNK and upstream JNK activating proteins generally inhibit chronic LV hypertrophy¹⁴⁻¹⁷. One JNK activating molecule, mixed lineage kinase 3 (MLK3) is a MAPKKK which is expressed ubiquitously¹⁸, though has not been investigated in cardiac function or remodeling. MLK3 contains an LZ domain and upon activation, stimulates JNK activation through direct regulation of MKK4 and MKK7. MLK3 also interacts with the Rho family GTPase CDC42¹⁹, which itself has been identified to inhibit pathologic LV hypertrophy after pressure overload¹⁴.

1.4 Central hypothesis.

In the present study, we tested the specific hypothesis that the molecule mixed lineage kinase 3 (MLK3) functions as a PKGI α anti-remodeling substrate. We tested a second related hypothesis that MLK3 is expressed in the human heart and becomes dysregulated in the failing and remodeled human heart. To test these hypotheses we performed: 1) molecular and cell culture studies to test the regulation of MLK3 by PKGI α ; 2) MLK3 protein expression studies in human heart tissue acquired from patients with no known heart disease, nonischemic cardiomyopathy, or inherited hypertrophic cardiomyopathy; and 3) *in vivo* studies in an experimental model of pressure overload-induced heart failure. We demonstrate that PKGI α binds to and activates MLK3 in cardiac tissue. We observe that inhibition of MLK3 kinase activity promotes cardiac myocyte hypertrophy in cell culture. We also demonstrate that pharmacologic inhibition of MLK3 prevents the activation of the anti-remodeling signaling pathways in cardiac myocytes. MLK3 protein expression increased more than 6 fold in left ventricular tissue

in patients with heart failure, and JNK expression increased by more than 10 fold in these tissues. Finally, in response to pressure overload induced by transaortic constriction surgery, mice with genetic deletion of MLK3 developed increased left ventricular hypertrophy, systolic dysfunction, and diastolic dysfunction, compared with wild type mice. Taken together, this study reveals for the first time that MLK3 functions an anti-remodeling signaling molecule, is expressed in the human heart, and becomes highly upregulated in the failing human heart. More broadly, these findings demonstrate that molecular studies to identify PKG substrates in the heart can reveal novel anti-remodeling mechanisms with translational relevance to human heart failure.

Materials and Methods

2.1 Regulatory approval.

All animal studies were performed in accordance with the Tufts University IACUC, protocol B2015-156. All human tissue samples were obtained under approval from the Tufts IRB protocol #9487.

2.2 Cell culture.

COS-1 cells were obtained from the American Type Culture Collection and cultured in Dulbecco's modified Eagle's medium (DMEM) (Invitrogen) supplemented with 10% fetal bovine serum, penicillin (100 units/ml), and streptomycin (100 µg/ml). Cells were grown at 37 °C in a 5% CO₂ humidified incubator.

2.3 cDNA Expression Plasmids.

Full-length WT and LZM PKGI α cDNA in a pCI plasmid were transiently transfected in COS-1 cells seeded in 6-well plates for 18 hours with Polyfect Transfection Reagent (Qiagen) using 1 µg plasmid cDNA per well. pGEX plasmids containing the

glutathione S-transferase (GST) tagged N-terminal amino acids 1-59 of PKGI α (WT: PKGI α 1-59) or the PKGI α LZ mutation (LZM: PKGI α LZM; containing multiple leucine or isoleucine to alanine mutations to disrupt LZ-dependent binding) were used as previously described¹¹. Human FLAG-tagged MLK3 cDNA was in a pCI plasmid.

2.4 Protein-protein interaction studies.

WT and LZM PKGI α were affinity purified from 250 μ g COS-1 whole cell protein lysates using cGMP immobilized agarose beads (Biolog) and rotated overnight at 4 $^{\circ}$ C. The cGMP-agarose beads were quickly washed three times in 500 μ L tissue lysis buffer (TLB: 20 mM HEPES, 50 mM β -Glycerol Phosphate, 2 mM EGTA, 1 mM DTT, 10 mM NaF, 1 mM NaVO₄, 1% Triton-X 100, 10% Glycerol, and supplemented with 1 mM PMSF). The cGMP-agarose beads were resuspended in TLB and incubated with 192 ng recombinant MLK3 (Invitrogen, PV3788) and rotated overnight at 4 $^{\circ}$ C. The protein-bead complexes were washed four times in TLB for 30 minutes per wash. The resulting protein-bead mixture was resuspended in 2X Laemmli Sample Buffer (Sigma) and assayed by western blot.

2.5 GST fragment interaction studies in mouse LV lysates.

GST pulldowns were performed as described (20). Hearts of C57/Bl6 male mice were rapidly excised and snap frozen in liquid nitrogen, followed by dounce homogenization of the left ventricle (LV) in lysis buffer as described previously^{11,20}. LV lysates were rocked gently overnight at 4 $^{\circ}$ C with fusion protein beads, followed by washing 3 times with lysis buffer. Proteins were eluted off the beads by boiling for 5 minutes in Laemmli sample buffer, followed by separation by SDS page and western blotting for MLK3. Equal loading of fusion proteins was confirmed by Coomassie stain.

2.6 Native immunoprecipitation of MLK3 from mouse LV lysates.

Left ventricular tissue from mice was acquired as described above, at a protein concentration of 1 mg/mL. After pre-incubation with protein G beads (GE Healthcare), supernatant was transferred to a new tube and incubated, overnight at 4°C, with anti-MLK3 antibody (Santa Cruz Biotechnology, Mouse Antibody), or with identical concentration of nonspecific IgG. The lysates were then incubated at 4°C with protein G for 45 mins followed by centrifugation at 1000g for 30 seconds and washing x 4 in lysis buffer. Proteins were denatured and separated for western blotting by SDS PAGE as described below.

2.7 Western blotting.

Cells were treated as described in the figure legends, rinsed in cold PBS, and lysed with TLB. Lysates were cleared by centrifugation and 20-50 µg of protein was used for western blotting. We used the following antibodies in this study: MLK3 (Cell Signaling Technology, 2817 and Abcam, ab51068), P-MLK3 Thr277/Ser281 (Abcam, ab191530), PKGI α ²⁰, P-JNK (Cell Signaling Technology, 4668), JNK (Cell Signaling Technology, 9252), GAPDH (Millipore, MAB374), and PDE5 (Cell Signaling Technology, 2395). Membranes were incubated with primary antibodies as per the manufacturer's recommendations and incubated with HRP-linked secondary anti-mouse or anti-rabbit antibodies (GE Healthcare, NA931 and NA934). Membranes were visualized using the ProteinSimple FluorChem E system and images were quantified using Alpha Innotech Imager software.

2.8 PKGI α target phosphorylation site prediction.

The human MLK3 protein (MAPKKK11, NCBI Reference Sequence: NP_002410.1) was entered into the NetPhosK 1.0 server (Center for Biological Sequence Analysis, Technical University of Denmark) to predict protein phosphorylation sites using an unfiltered analysis with a minimum score threshold of 0.50²¹.

2.9 Kinase reactions.

Purified PKGI α protein (Promega V517A) and recombinant MLK3 protein were diluted in resuspension buffer (20 mM HEPES, 1 mM DTT, and 0.33% Brij-35) and then incubated in kinase assay buffer (20 mM HEPES, 1 mM DTT, 5 mM MgCl₂, and 0.1 mM ATP). Proteins were incubated at 30 °C for 30 minutes and the reaction was quenched by addition of 2X Laemmli Sample Buffer.

2.10 Cell Culture Studies.

Cell studies of PKGI α phosphorylation of MLK3 were performed in HEK293 cells. Briefly, 8 mg of MLK3 harboring a C-terminal Flag epitope tag (MLK3-FL) in pCI plasmid was incubated for 21 hours with HEK293 cells grown on 100mm plates, using Qiagen Polyfect reagent. At 21 hours after transfection, cells were treated with 5 mM 8Br-cGMP at 37 °C for 30 minutes, followed by lysis on ice as described²⁰. MLK3 immunoprecipitation was performed with anti-Flag antibody (Cell Signaling) followed by western blot for phospho-MLK3 as described above.

2.11 Adult mouse cardiomyocyte (AMCM) culture.

All rodent care was in accordance with and approved by the Institutional Animal Care and Use Committee of Tufts University School of Medicine and Tufts Medical Center. AMCMs were isolated as previously described²². For siRNA experiments, AMCMs were incubated with siRNA directed against MLK3 (Santa Cruz, sc-35946) or a

control non-targeting siRNA (Santa Cruz, sc 37007) with delivery platform (Santa Cruz transfection medium) for 48 hrs prior to treatment as indicated in the figure legends.

2.12 Adult rat ventricular myocyte (ARVM) culture.

ARVMs were isolated as previously described²³ from 175-200g adult male Sprague-Dawley rats (Envigo). For signaling experiments ARVMs were plated at a non-confluent density of 50 cells/mm² on p60 dishes coated with mouse laminin (Invitrogen). After 1 hr of plating the media was replaced and for signaling experiments the cells were used the following day. For CM size measurements, ARVMs were plated on laminin-coated glass coverslips and after 1 hr the media was replaced with fresh media containing either DMSO vehicle (diluted 1:10,000 in media) or the MLK3 inhibitor URM-099 (Selleckchem) diluted in DMSO to 100 nM. After 48 hrs of incubation the cells were fixed and stained with Alexa-Fluor 488 Phalloidin (Life Technologies) according to the manufacturer's recommendations. Coverslips were mounted on slides with solution containing DAPI (Life Technologies) and visualized by fluorescent microscopy. CM size was measured from images using Image-Pro Software (Version 6.2, MediaCybernetics). For each experiment 20-50 cells were measured per treatment condition.

2.13 Experimental animals.

Whole body MLK3 knockout mice (denoted MLK3^{-/-}, originally described²⁴) and MLK3 WT littermates (denoted MLK3^{+/+}) on the C57Bl6 background were obtained from breeding MLK3-heterozygote mice. Investigators were blinded to animal genotype during the animal surgeries through the subsequent data analysis.

2.14 Transthoracic echocardiography

Mice were anesthetized with 2.5% isoflurane and M-Mode images were acquired from the mid-papillary short-axis view as described previously¹¹. Fractional shortening was calculated using the following standard equation: $FS\% = ([EDD - ESD] / EDD) \times 100$.

2.15 Transaortic constriction.

Body weight and age-matched littermate mice were randomly assigned to either sham or transaortic constriction (TAC) surgery. TAC was performed as previously described^{11,25} with a 25-gauge needle used to size the ligature around the transverse aorta.

2.16 LV *in vivo* hemodynamic measurements.

After 7 days of TAC or sham surgery, mice were anesthetized with 2.5% isoflurane and hemodynamic analyses were performed using a pressure-volume transducing catheter as described¹¹. Hemodynamic data were recorded and analyzed using IOX Software (EMKA version 2.1.10).

2.17 Histological analysis.

The LV was fixed in 10% formalin, embedded in paraffin, cut into 4- μ m sections and stained with hematoxylin and eosin for CM size measurements and picrosirius red to assess cardiac fibrosis. For CM size measurements, CMs from mid-papillary sections with central nuclei were traced using Image-Pro and 50 myocytes were quantified per LV sample. For interstitial fibrosis measurements, picrosirius red positive staining was calculated as a percentage of the total tissue area per image. For perivascular fibrosis measurements the percent of picrosirius red positive staining was calculated was normalized to vessel size.

2.18 qRT-PCR analysis.

Mouse LV total RNA was extracted using Trizol (Invitrogen) and 1 µg of RNA was reverse transcribed to cDNA using the QuantiTect Reverse Transcriptase Kit (Qiagen). Target primers and cDNA samples were incubated in a 384-well plate in triplicate and amplified by quantitative real-time PCR using Ssofast Evagreen Supermix (Biorad) for 40 cycles performed at 95 °C for 15 seconds and 60 °C for 1 minute using an ABI Prism 7900 Sequence Detection System (Applied Biosystems).

2.19 Human heart samples.

Normal donor hearts were obtained from the National Disease Research Interchange (NDRI). Tissue from patients with nonischemic cardiomyopathy was obtained from two sources. First, in patients undergoing surgical implantation of left ventricular device for end stage HF, apical tissue removed for insertion of the inflow cannula was placed immediately on ice, partitioned into segments, then snap frozen and stored. Additional heart tissue was obtained in the same manner from explanted hearts in patients with end stage NICM undergoing heart transplant. Tissue from symptomatic hypertrophic cardiomyopathy patients was obtained from septal tissue removed during LV septal reduction surgery. Tissue banking protocols were approved by the Tufts Medical Center Internal Review Board (IRB#9487). Positive controls for western blotting human lysates were purchased from Cell Signaling, Inc.

2.20 Statistical Methods.

Analysis of two group comparisons was performed by 2 tailed unpaired Student's t test. Data from *in vivo* experiments were analyzed by 2-Way ANOVA controlling for genotype and surgery, with multiple comparison testing by Student-Newman-Keuls Method.

2.21 Statistical analysis of protein expression from human heart samples.

Target sample numbers for these experiments were determined under several assumptions. First, we predicted that we would be able to detect a 50% difference in ADUs between normal and failing hearts. We set our control (normal donor) densitometry value to 1.0 ADUs, meaning that we would assume that the difference between control and failing hearts would exceed 0.5 ADUs. Because no studies had previously measured MLK3 protein levels in failing human hearts, we assumed this conservative estimate for protein difference based on published literature on other proteins which are expressed differentially in failing versus normal hearts²⁶. This estimate is conservative because most proteins that play a role in the hypertrophy process differ by at least two-fold when measured in failing hearts versus normal hearts. In calculating power, we also assumed a standard deviation σ of 0.5. This again was based on published literature²⁶. Third, we predicted that samples would have a normal distribution of ADUs and thus we will be able to compare the means. Therefore in order to detect the above difference in means at the assumed σ , and with a β error of 0.1 and α error of 0.05, we required 23 samples per experimental group.

Analysis of protein expression from human heart samples was compared by ANOVA with multiple comparison testing. All data shown represent the results obtained from independent experiments conducted with multiple replicates (as noted in the figure legends) with standard error of the mean (mean \pm SEM). Values of $p < 0.05$ were considered statistically significant.

Results

3.1 PKGI and MLK3 co-interact in the LV.

To investigate PKGI α LZ-dependent interactions in the myocardium, GST-fusion proteins containing the PKGI α LZ domain were incubated with mouse LV lysates, and western blotting was performed for MLK3. We detected MLK3 protein in the precipitant from PKGI α LZ domain fusion proteins (amino acids 1-59), but not with GST alone or with mutant LZ domain¹⁰ containing disrupting leucine to alanine mutations (Figure 2). Immunoprecipitation of native MLK3 from mouse LV lysates co-precipitated full length PKGI α , but control IgG immunoprecipitation precipitated no detectible MLK3 or PKGI α . To test for a direct interaction of PKGI α and MLK3, we transfected Cos1 cells with WT or LZ mutant PKGI α , and affinity purified PKGI α , followed by incubation with recombinant MLK3. MLK3 precipitated with WT PKGI α , but to a lesser degree with the LZ mutant PKGI α , indicating direct binding of PKGI α and MLK3 and also indicating the requirement of the PKGI α LZ domain for this interaction.

3.2 PKGI α induction of MLK3 phosphorylation.

Analysis of the MLK3 sequence by the Group-based phosphorylation scoring (GPS) program identified a PKGI α GPS score of

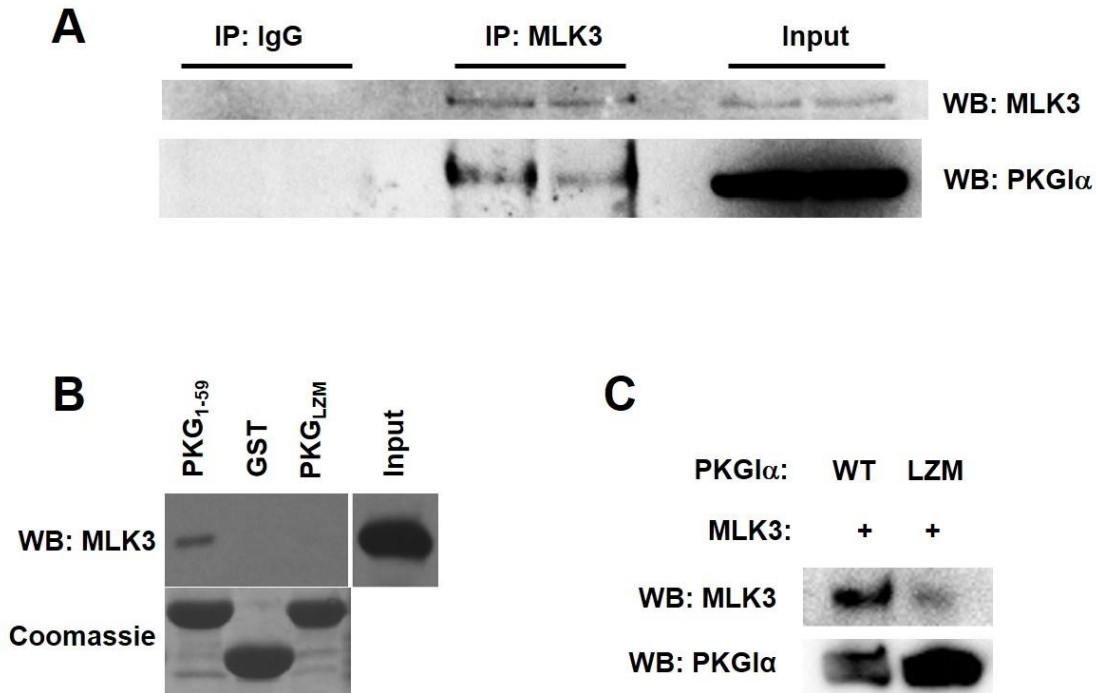


Figure 2. PKGI α interacts with MLK3 in LZ-dependent manner. (A) Co-immunoprecipitation of native MLK3 with native PKGI α from mouse left ventricular lysate was evaluated by western blotting for PKGI α . Western blotting for MLK3 was used to confirm immunoprecipitation (n=5). (B) Co-precipitation of the GST-tagged N-terminal PKGI α LZ domain (amino acids 1-59) with native MLK3 from mouse left ventricular lysate was evaluated by western blotting for MLK3. Coomassie staining was used to confirm total protein input of the GST-tagged proteins (n=3). (C) Full length PKGI α WT or LZM were affinity purified from transfected Cos1 cells and incubated with recombinant MLK3. Co-precipitation of recombinant MLK3 was detected by western blotting. (n=4) For all of these experiments each replicate is an independent experiment; LZM = Leucine Zipper Mutation, WB = western blot, NS = non-specific.

0.51 on Ser281 of MLK3, indicating high likelihood of PKGI α phosphorylation on this residue (Figure 3). Previous studies have identified that phosphorylation of Ser281 and Thr277 activate MLK3 kinase activity²⁷. We therefore tested the direct effects of cGMP

and PKG on MLK3 phosphorylation. In HEK293 cells transfected with MLK3,

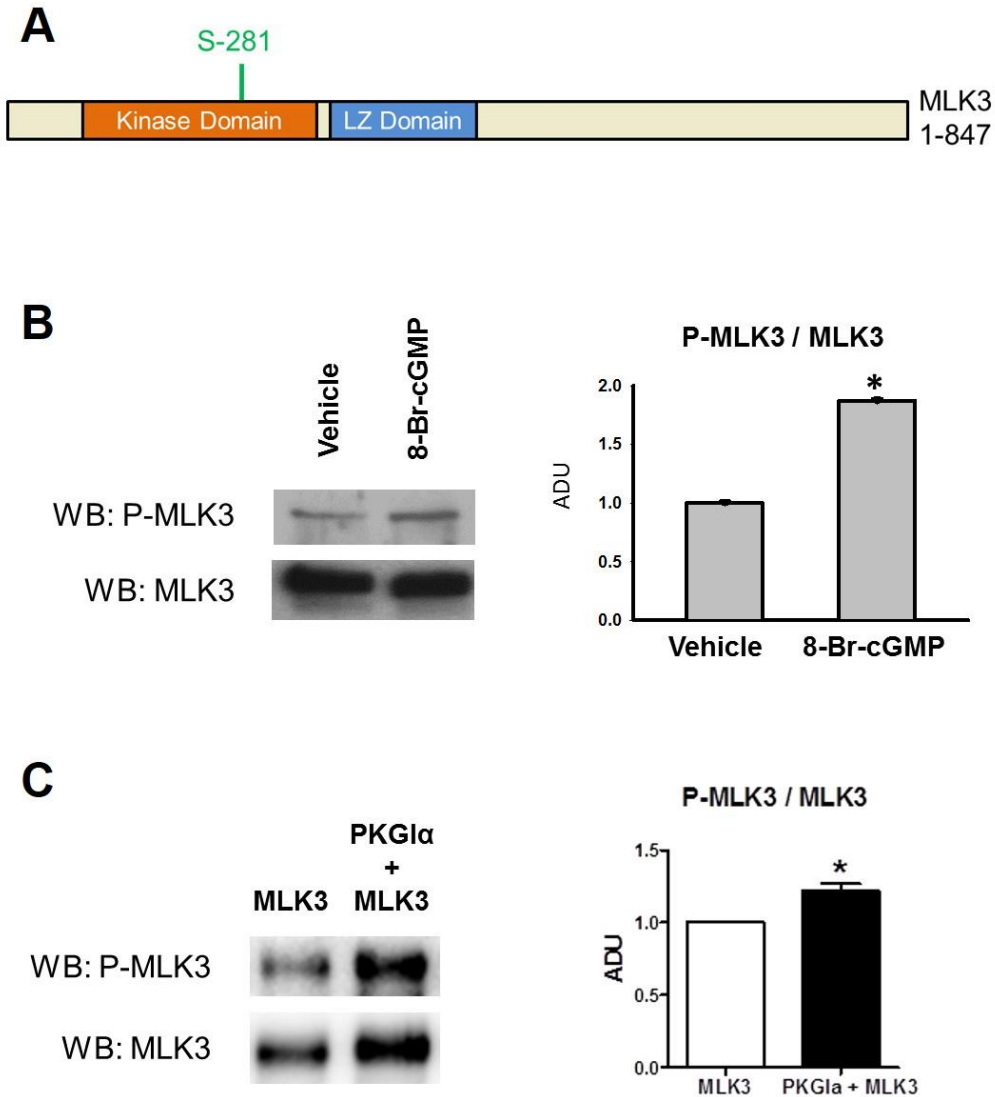


Figure 3. PKGI α stimulates MLK3 phosphorylation on the activation loop residues Thr-277 / Ser-281. (A) Analysis of PKGI α target sites on MLK3 using NetPhosK 1.0 reveals a potential phosphorylation site Ser281 within the MLK3 kinase domain. (B) HEK 293 cells transfected with FLAG-tagged MLK3 were stimulated with 8-Bromo-cGMP (8-Br-cGMP, 5mM, 30 minutes) or vehicle. Immunoprecipitants from cell lysates were western blotted for phosphorylation of MLK3 (P-MLK3) on residues Thr-277/Ser-281. Western blotting data was quantified by densitometry, normalized to total MLK3, and expressed relative to vehicle treated cells (n=3, student's unpaired T-test). (C) Phosphorylation of recombinant MLK3 on residues Thr-277/Ser-281 was assessed in a kinase reaction mixture containing recombinant MLK3 and PKGI α proteins. Levels of phosphorylated MLK3 were quantified by densitometry, normalized to total MLK3, and expressed relative to recombinant MLK3 incubated alone (n=3, student's paired T-test). For all of these experiments each replicate is an independent experiment; * = p < 0.05, and error bars are mean \pm standard error.

the PKGI activator 8-Bromo-cGMP increased MLK3 phosphorylation as detected with a MLK3 Thr277/Ser281 phospho-specific antibody (Figure 3). Purified PKGI α also directly increased phosphorylation on these sites when incubated with recombinant MLK3.

Because PKGI has previously been demonstrated to activate JNK signaling in the CM²⁸ we next tested the requirement of MLK3 for PKG-induced JNK activation in the CM. In isolated CMs, 8-Br-cGMP induced JNK phosphorylation (Figure 4), consistent with other published observations²⁸. However, siRNA silencing of MLK3 abolished this effect, supporting the requirement of MLK3 for the 8-Br-cGMP activation of JNK.

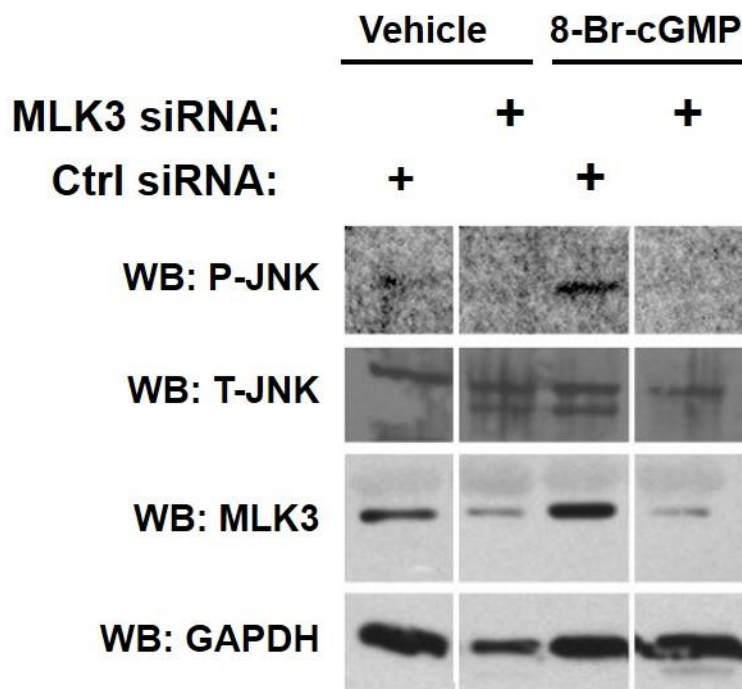


Figure 4. MLK3 is required for cGMP-induced JNK phosphorylation in cardiomyocytes. (A) Mouse cardiomyocytes were transfected with siRNA to deplete MLK3 (80 nM, 48 hrs) and then stimulated with 8-Bromo-cGMP (8-Br-cGMP, 100 μ M, 60 mins). JNK activation was measured by western blot (n=3).

3.3 Inhibition of MLK3 kinase activity represses JNK activation in the cardiac myocyte and promotes cardiac myocyte hypertrophy.

We next investigated the effects of MLK3 kinase inhibition on isolated cardiac myocytes. In adult rat ventricular myocytes (ARVM), the MLK3 inhibitor URM-099²⁹ decreased basal JNK phosphorylation (activation) in a dose-dependent manner (Figure 5), supporting that MLK3 normally maintains CM JNK phosphorylation through kinase activity. H₂O₂, which potently induces JNK activity³⁰, increased CM JNK phosphorylation in ARVMs. However, URM-099 completely inhibited H₂O₂-induced JNK phosphorylation in these cells. Administration of URM-099 for 48 hours to ARVMs induced CM hypertrophy (1 ± 0.02 arbitrary units in DMSO vehicle versus 1.27 ± 0.04 arbitrary units in URM-099 treated) (Figure 5). Interestingly, URM-099 had no effect on phenylephrine-induced CM hypertrophy (not shown). These findings support that MLK3 kinase activity can represses CM hypertrophy.

3.4 MLK3 expression increases in the pressure overloaded LV, and in the failing human LV.

To test the potential *in vivo* relevance of MLK3 to cardiac hypertrophy and remodeling, we measured MLK3 expression in the mouse LV after 7 days of pressure overload by transaortic constriction (TAC). Normalized MLK3 expression increased nearly 2-fold by day 7 after TAC (Figure 6). We next examined MLK3 and JNK expression in LV tissue from patients with end-stage nonischemic cardiomyopathy (NICM), or hypertrophic cardiomyopathy (HCM) undergoing surgical septal myectomy. Compared with normal human donor LV tissue from the national disease research

interchange (NDRI), MLK3 expression significantly increased in both NICM and HCM LVs (fold increase vs. normal control 3.26 ± 0.86 ADU in NICM; 6.97 ± 1.42 ADU in

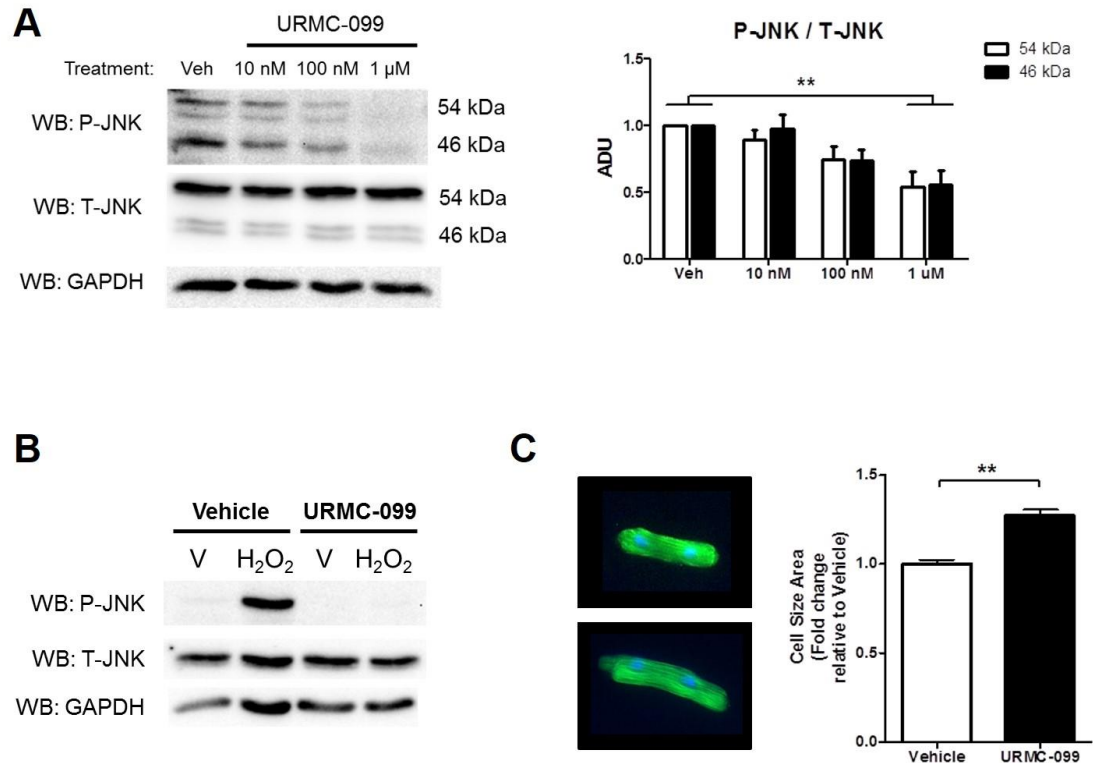


Figure 5. Inhibition of MLK3 kinase activity blocks JNK activation in the cardiac myocyte and causes cardiac myocyte hypertrophy. (A) ARVMs were pretreated with vehicle (DMSO) at a 1:10,000 concentration or the MLK3 inhibitor URM-099 (10 nM, 100 nM, or 1 μ M) for 60 minutes. The phosphorylation of JNK (54 kDa and 46 kDa) was quantified and expressed relative to total JNK (54 kDa and 46 kDa) (n=4, 1 Way ANOVA, Bonferroni's post-test ** = p < 0.01). (B) ARVMs were pretreated with vehicle (DMSO) as in (A) or the MLK3 inhibitor URM-099 (1 μ M) for 60 minutes prior to stimulation with vehicle (H₂O) or H₂O₂ (100 μ M, 60 minutes). (C) ARVMs were treated with either vehicle (DMSO) or URM-099 (100 nM) for 48 hrs, followed by phalloidin staining. Cell area was quantified directly and expressed as fold change relative to vehicle treated cells (n=4, student's T-test). For this experiment each replicate is an independent experiment from separate cardiomyocyte preparations; ** = p < 0.01, and error bars are mean \pm standard error. V = vehicle.

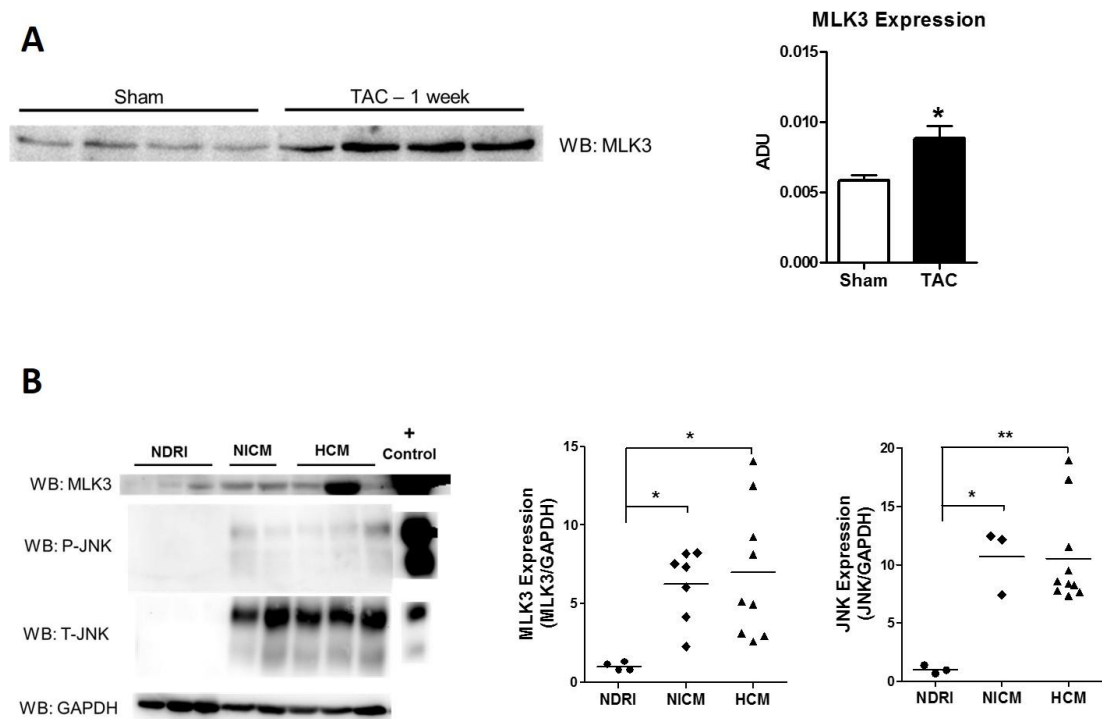


Figure 6. MLK3 expression is increased in the left ventricle after pressure overload, and in the human failing left ventricle. (A) LV lysates from wild type mice subjected either to sham or transaortic constriction (TAC) for 7 days were subjected to western blot for MLK3, and expression was normalized to actin band on Ponceau stain. (B) Human LV tissues samples from non-diseased donors (NDRI), non-ischemic cardiomyopathy (NICM), or hypertrophic cardiomyopathy (HCM) patients were evaluated by western blot for MLK3, P-JNK, T-JNK, and GAPDH (n=4-9 per group). Also shown is summary data of MLK3 and JNK expression quantified by densitometry and normalized to GAPDH. Data were analyzed by ANOVA and are expressed as mean \pm standard error; * = $p < 0.05$, ** = $p < 0.01$; comparisons are denoted in the figures.

HCM). JNK expression also increased to a significant degree in both NICM and HCM, compared with normal donors (fold increase vs. normal control 10.68 ± 1.64 ADU in NICM; 10.53 ± 1.33 ADU in HCM). JNK phosphorylation, determined as phosphorylated/total JNK, trended toward increased in NICM and HCM tissue.

Expression of PDE5, which has previously been shown to increase in end-stage cardiomyopathy²⁶ also increased significantly in the NICM and HCM samples (fold increase vs. normal control 25.33 ± 3.99 ADU in NICM; 35.27 ± 9.82 ADU in HCM).

3.5 MLK3 deletion leads to increased LV dysfunction and hypertrophy after pressure overload.

To test the role of MLK3 in the cardiac remodeling response *in vivo*, we studied the cardiac phenotype in mice with whole body deletion of MLK3. These MLK3 knockout (MLK3^{-/-}) mice are fully viable and have normal lifespan²⁴. Baseline examination of cardiac structure in 3 month old male MLK3^{-/-} mice revealed mild LV and cardiac hypertrophy, compared with littermate MLK3^{+/+} controls (Table 1). Echocardiographic parameters, however, did not differ between genotypes. To test the role of MLK3 on the cardiac remodeling response, we next subjected 10-12 week old male MLK3^{-/-} mice to LV pressure overload by transaortic constriction (TAC) for 7 days, followed by invasive hemodynamic analysis and organ harvest. Aortic systolic pressure did not differ between MLK3^{+/+} and MLK3^{-/-} TAC mice, indicating induction of similar degrees of pressure overload between groups (Figure 7B). However, compared with MLK3^{+/+} TAC mice, MLK3^{-/-} TAC hearts developed elevated LV end diastolic pressure, which is a hallmark of LV failure. The LV pressure recordings from MLK3^{-/-} TAC hearts also displayed decreases in dP/dt_{max} and dP/dt_{min} , compared with MLK3^{-/-} sham controls, indicating systolic and diastolic function, respectively. These parameters did not decrease significantly in MLK3^{+/+} controls. Additional measures of LV systolic function, ejection fraction and preload recruitable stroke work, decreased significantly in MLK3^{-/-} hearts,

compared with MLK3^{+/+} controls, further indicating deterioration of cardiac function with deletion of MLK3. In addition to the functional abnormalities described above,

	MLK3 ^{+/+}	MLK3 ^{-/-}	P
Organ Weights	(n=11)	(n=14)	
LV (mg)	83.5 ± 2.6	99.4 ± 3.1 †	0.0009
HW (mg)	114.1 ± 3.2	127.9 ± 3.7 *	0.0117
LV/TL (mg/cm)	47.1 ± 1.5	57.2 ± 1.8 †	0.0003
HW/TL (mg/cm)	64.4 ± 1.9	73.6 ± 2.1 **	0.0043
BW (g)	29.3 ± 1.2	28.4 ± 0.8	0.5636
Echocardiography	(n=9)	(n=7)	
EDD (mm)	3.34 ± 0.12	3.67 ± 0.15	0.1047
ESD (mm)	2.01 ± 0.15	2.29 ± 0.18	0.2398
AWT (mm)	0.97 ± 0.06	1.16 ± 0.12	0.1627
PWT (mm)	1.07 ± 0.10	1.19 ± 0.12	0.4634
FS%	40.3 ± 2.9	38.2 ± 2.8	0.6110
HR (s⁻¹)	460 ± 17	433 ± 26	0.3834

Table 1. Baseline organ masses and echocardiographic data in MLK3^{+/+} and MLK3^{-/-} mice. Organs from mice at 12 weeks of age were weighed and normalized relative to tibia length. Data were analyzed by ANOVA and are expressed as mean ± standard error; * = p < 0.05, ** = p < 0.01, † < 0.001 vs MLK3^{+/+} mice. LV = left ventricle; HW = heart weight; TL = tibia length; BW = body weight; EDD = End diastolic diameter; ESD = End systolic diameter; AWT = Anterior wall thickness; PWT = Posterior wall thickness; FS = Fractional shortening; HR = heart rate.

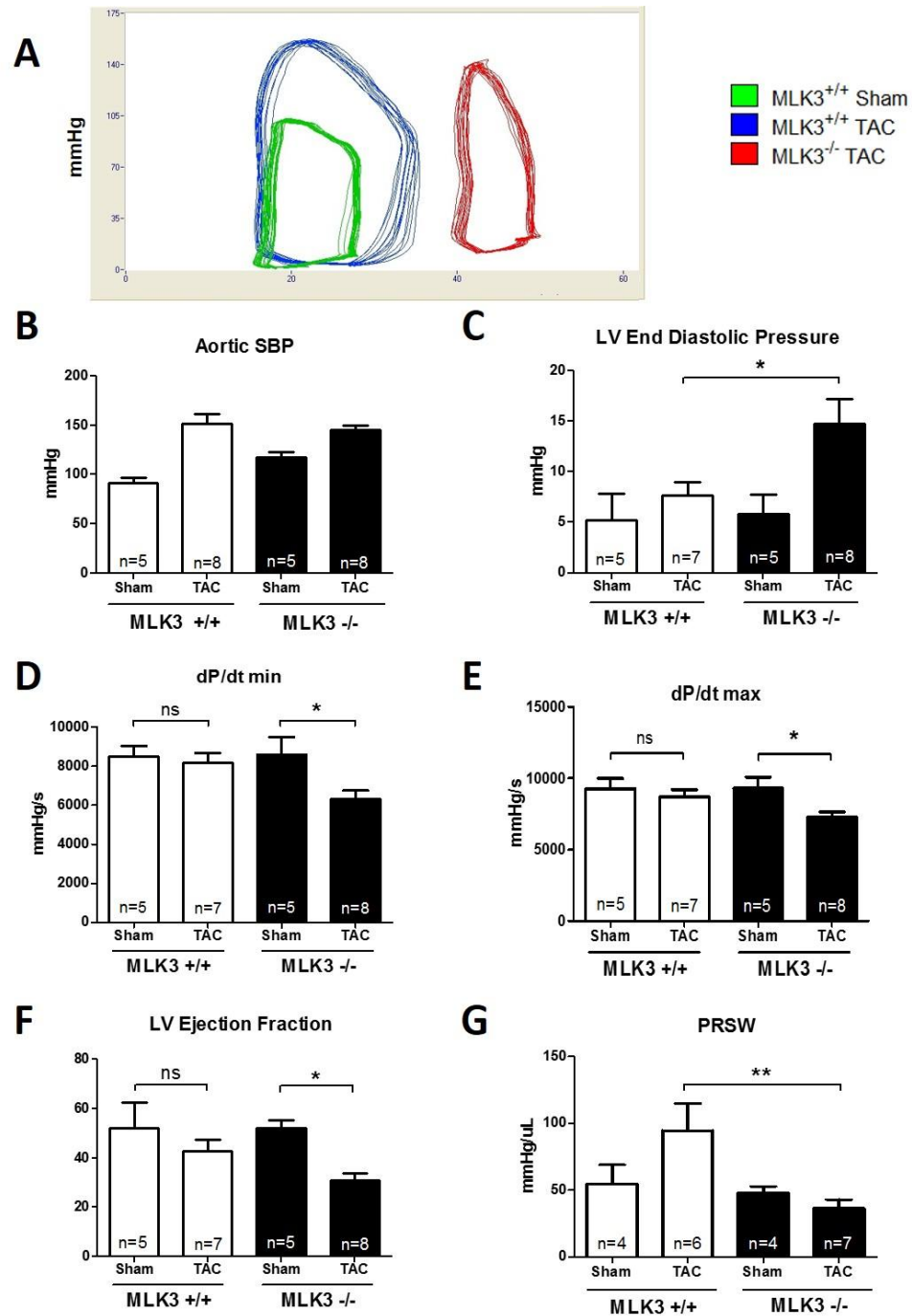


Figure 7. MLK3^{-/-} mice develop increased cardiac dysfunction after pressure overload. LV function was evaluated by *in vivo* hemodynamics in MLK3^{+/+} and MLK3^{-/-} subjected to sham or TAC surgery for 7 days. (A) Representative pressure-volume relationship loop in TAC MLK3^{+/+} and MLK3^{-/-} mice. (B) Systolic blood pressure (SBP) was measured in the aorta proximal to the TAC ligature (n=5-8 per group). (C) LV End Diastolic Pressure (LVEDP). (D) Peak rate of rise of LV pressure (dP/dT max). (E) Peak rate of lowering of LV pressure (dP/dT min). (F) LV Ejection Fraction (LVEF). (G) Preload Recrutable Stroke Work (PRSW). Data were analyzed by 2-way ANOVA and are expressed as mean ± standard error; * = p < 0.05; ** = p < 0.001. Comparisons are denoted in the figures.

MLK3^{-/-} TAC LVs had increased normalized mass compared with MLK3^{+/+} LVs (Figure 8). Expression of the fetal gene *nppa* increased significantly in MLK3^{-/-} TAC LVs, compared with MLK3^{+/+} TAC LVs, supporting pathological, rather than physiological, hypertrophy in the MLK3^{-/-} hearts. LV interstitial fibrosis, assessed by picrosirius red staining, did not differ between TAC genotypes, and was not increased in TAC compared with sham LVs at the 7 day time point. However, mRNA expression of the collagen gene *coll1a1* increased significantly in the MLK3^{-/-} TAC LVs, compared with MLK3^{+/+} TAC controls, supporting a pro-fibrotic gene expression pattern selectively in the MLK3^{-/-} TAC response.

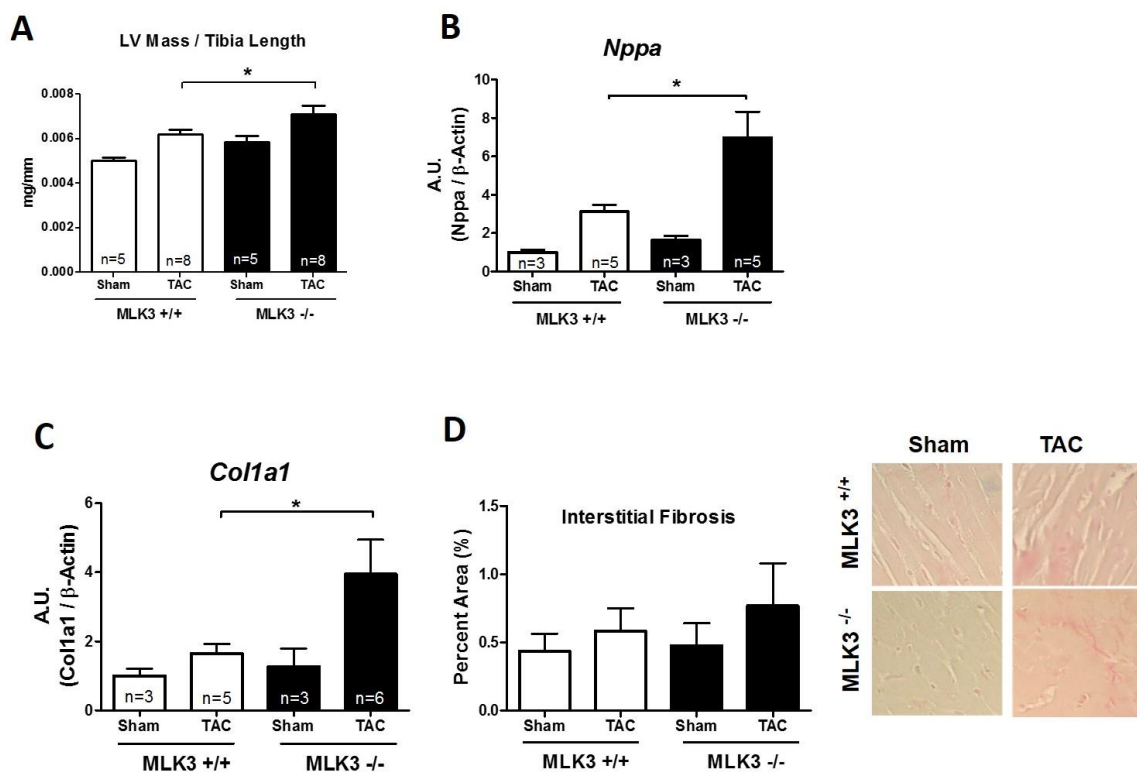


Figure 8. MLK3^{-/-} mice develop increased pathologic LV hypertrophy and fibrotic gene expression after pressure overload. MLK3^{+/+} and MLK3^{-/-} mice subjected to sham or TAC surgery for 7 days were evaluated for (A) LV mass corrected for tibia length (n=6-8 per group). (B) qRT-PCR analysis of LV *Nppa* gene expression normalized to β -Actin (n=3-6 per group). (C) qRT-PCR analysis of LV *Col1a1* gene expression normalized to β -Actin (n=3-6 per group). (D) Summary and representative histological analysis of picrosirius red stained LV sections (n=3-6 per group) Data were analyzed by ANOVA and are expressed as mean \pm standard error; * = $p < 0.05$, ** = $p < 0.01$; comparisons are denoted in the figures.

Discussion and Future Directions

In the present study we tested the hypothesis that MLK3 functions as a myocardial PKGI α LZ-dependent binding substrate and anti-remodeling molecule. We demonstrated that: 1) the MAPKKK MLK3 interacts with PKGI α in the LV, through mechanisms requiring an intact PKGI α LZ domain; 2) PKGI α induces phosphorylation of the MLK3 kinase activation site both in cell culture and *in vitro*; 3) MLK3 kinase inhibition in cardiac myocytes inhibits tonic JNK activation and promotes CM hypertrophy; 4) MLK3 expression increases highly in the failing human LV; and 5) genetic deletion of MLK3 leads to increased pathologic cardiac remodeling in response to LV pressure overload. Taken together, these findings support that MLK3 functions as a novel PKGI α effector and anti-remodeling molecule, is required for JNK activation in the myocardium, is expressed in the human heart and becomes upregulated in the failing human LV. Further, this study supports the broader concept that myocardial PKGI α leucine-zipper binding substrates function as anti-remodeling molecules.

4.1 Leucine zipper dependent binding of PKGI α and MLK3.

PKGI α is a serine/threonine kinase, which means that it enzymatically adds phosphates to substrate proteins either on serine or on threonine amino acids. Although there are many intrinsic serine/threonine kinases, they differ in the molecules that they phosphorylate because their molecular structures differ, thus enabling selective phosphorylation of particular substrates by individual kinases. In order to phosphorylate a substrate, kinases must either directly bind to that substrate or bind to adapter proteins which help co-localize the protein with the substrate. For those reasons, we hypothesized that identifying molecules that PKGI α interacts with could prove a useful strategy to

define new PKGI α phosphorylation targets, which by extension could reveal novel mechanisms regulating cardiac remodeling. We initially identified MLK3 as a PKGI α -binding partner by screening for myocardial proteins selectively interacting with the PKGI α LZ domain. In the vascular smooth muscle cell, where it has been more extensively studied, the PKGI α LZ domain mediates PKGI α binding to important substrates, including myosin light chain phosphatase¹⁰, regulator of G protein signaling²³¹, RhoA²⁰, and formin homology domain 1³². Binding of PKGI α to these substrates enables PKGI α to phosphorylate them, thereby changing their function and inducing vasodilation. Our current studies demonstrate that MLK3 precipitates with the PKGI α LZ domain but not with mutant LZ domain in cardiac lysates, supporting an LZ-dependent interaction of MLK3 with PKGI α in myocardial tissue. In addition, our immunoprecipitation studies have identified that MLK3 co-precipitates with full length native PKGI α in the heart. Further, purified WT PKGI α , but not LZ mutant PKGI α , selectively precipitates with recombinant MLK3 *in vitro*. Taken together, we interpret these studies to identify that PKGI α and MLK3 directly bind in myocardial tissue through interaction mediated by the PKGI α LZ domain.

The co-interaction of PKGI α with MLK3 led us to investigate further its regulation by PKGI α and its potential role in cardiac remodeling. MLK3 was first identified and cloned as a kinase possessing sequence homology with both serine/threonine and tyrosine kinases¹⁸. Subsequent investigations demonstrated MLK3 to be ubiquitously expressed¹⁹, and part of a family of mixed lineage kinases which function as upstream MAPKKKs and predominantly activate JNK pathway signaling¹⁹. MLK3 contains an internal LZ domain with high sequence homology to PKGI α ¹⁸. MLK3

kinase activity is activated upon phosphorylation of thr277 and ser281, either by other kinases¹⁹ or through autophosphorylation induced by interaction with the Rho GTPase CDC42¹⁹. Our observations that incubation of MLK3 with PKGI α increased MLK3 thr277/ser281 phosphorylation support that PKGI α directly activates MLK3 kinase activity. Our cell culture studies showing that 8-Br-cGMP increases MLK3 phosphorylation further support that this activation occurs in cells as well as *in vitro*. However, whether PKGI α directly phosphorylates MLK3 on these sites, or whether PKGI α rather induces MLK3 autophosphorylation solely by promoting conformational changes in MLK3, remains unknown.

4.2 Regulation of MLK3 expression in the failing LV.

As part of our overall experimental strategy, we initially performed molecular screens for PKGI α binding proteins for the reasons described above. Before undertaking extensive investigation of these proteins, however, we first wanted to test the relevance of these proteins to humans and to human heart failure. For these reasons we investigated whether MLK3 is expressed in human heart tissue, and whether its expression changes in the failing human heart, which would in turn support that it is regulated in the heart under disease conditions. Our findings reveal, for the first time, that MLK3 is expressed in the human LV, and importantly, that MLK3 expression increases in the failing LV. We detected low level MLK3 expression in normal human LV tissue, providing the first evidence of MLK3 protein expression in the human heart. Moreover, we observed significantly elevated MLK3 expression in both nonischemic cardiomyopathy and in hypertrophic cardiomyopathy tissue in humans, supporting that MLK3 expression is upregulated in end stage HF and in structural remodeling, respectively. In order to

measure the regulation of MLK3 expression in a more controlled experimental HF model, we measured MLK3 protein expression in hearts of LV pressure overloaded (TAC) mice, and again observed increased MLK3 expression compared with sham controls. It should be noted that although protein expression of MLK3 increased in both HCM and NICM, these observations do not indicate whether MLK3 activity, localization, and posttranslational modifications may become altered in the failing ventricle. These findings do strongly support, however, the relevance of MLK3 to the human heart and to heart failure, and support further investigation into the mechanisms by which MLK3 regulates these processes.

The finding that MLK3 and JNK expression become increased in HCM is of specific interest, as the molecular signaling cascades regulating hypertrophic remodeling in HCM remain poorly understood. HCM arises from mutations of sarcomeric proteins³³. However, the phenotypic effects of these mutations vary in their penetrance³⁴, and recent data supports that intracellular signaling molecules may modify the effects of these mutations³⁴. Therefore we speculate that PKGI signaling through MLK3 may modulate the cardiac phenotype in HCM, though this hypothesis admittedly remains untested.

4.3 MLK3 promotes JNK phosphorylation and inhibits CM hypertrophy.

Though our MLK3 expression data in human tissue support the relevance of MLK3 to HF, they do not indicate whether MLK3 normally opposes, promotes, or only represents a marker of, cardiac remodeling. We therefore investigated MLK3 regulation of JNK, as the JNK signaling pathway directly regulates cardiac remodeling and failure. Initial investigations by others demonstrated that JNK induced cell growth in cultured neonatal myocytes, suggesting that it normally may promote adverse cardiac

remodeling³⁵. However, multiple reports over the past decade have supported the contrasting notion that JNK generally opposes the initial development of stress-induced cardiac hypertrophy and dysfunction. Specifically, genetic deletion studies of upstream JNK activators such as CDC42¹⁴, MEKK1¹⁷, MKK4¹⁶, and MKK7¹⁵ have identified a requirement of these genes for normally repressing stress-induced cardiac hypertrophy and remodeling, in some cases through specific roles in the CM¹⁴⁻¹⁶. Further, genetic deletion of JNK isoforms impairs the initial LV compensatory response to pressure overload and induces progressive cardiac hypertrophy^{12,13}. Thus JNK pathway activation can inhibit cardiac remodeling and dysfunction. PKGI α activates JNK signaling in the CM through unknown mechanisms²⁸. Further, PKGI α LZ mutant mice, which develop severe LV dysfunction and mortality after TAC¹¹, also display markedly blunted JNK activation as early as 48 hours after TAC, supporting that PKGI normally activates JNK pathway signaling through LZ-dependent effectors, and further that disruption of JNK in the LZM hearts may contribute to this adverse phenotype¹¹. In the present study, we observed that pharmacological MLK3 inhibition in adult CMs reduced both basal as well as H₂O₂-induced JNK phosphorylation. Further, our knockdown experiments demonstrate that reduction of MLK3 expression leads to decreased cGMP-induced JNK phosphorylation in CMs. Taken together these findings support that MLK3 functions as a JNK activating molecule in the CM, and mediates activation of JNK by PKGI in the CM. We also interpret our findings to support that understanding PKGI α LZ-dependent regulation of the JNK pathway in the heart may reveal novel anti-remodeling pathways, such as the MLK3 signaling pathway.

4.4 Role of MLK3 in the LV response to pressure overload *in vivo*.

Our experiments in MLK3^{-/-} mice identify for the first time that MLK3 represses pressure overload-induced cardiac hypertrophy and dysfunction *in vivo*. Our finding of basal LV hypertrophy in MLK3^{-/-} mice was unexpected, and suggests a role of MLK3 as a tonic inhibitor of LV hypertrophy. Although our cultured CM data support that MLK3 kinase activity represses basal CM growth, whether the baseline LV hypertrophy in MLK3^{-/-} mice arises from intrinsic CM abnormalities versus extrinsic effects remains unknown. Regardless, our TAC experiment demonstrated further increased LV hypertrophy as well in MLK3^{-/-} compared with MLK3^{+/+} controls. More striking, however, were the functional decrements which occurred in the MLK3^{-/-} mice subjected to LV pressure overload. We interpret these findings to support that MLK3 normally mediates LV functional compensation to pressure overload. Further, our observations that MLK3 is required for preservation of LV function after TAC correlates with previous published data demonstrating a role for both PKGI α and JNK in mediating the initial functional compensation of the LV to pressure overload^{11,12}. Our findings of increased fetal gene expression and collagen gene expression in MLK3^{-/-} TAC hearts provide additional evidence that MLK3 normally opposes the maladaptive gene expression changes which contribute to cardiac remodeling. Although overt interstitial fibrosis did not differ between MLK3^{-/-} and MLK3^{+/+} TAC hearts, we made these observations at a relatively early experimental time point (7 days) in which advanced fibrosis does not yet occur. Our gene expression data showing increased collagen expression in MLK3^{-/-} TAC hearts, do suggest an early pro-fibrotic phenotype in these mice.

4.5 Clinical relevance of MLK3 as novel regulator of cardiac remodeling.

Understanding PKGI α anti-remodeling effectors is of substantial clinical relevance, since PKGI-activating drugs remain under active investigation in HF⁵. Recently, for example, the PARADIGM-HF trial⁶ demonstrated the superiority of neprilysin inhibition combined with angiotensin receptor blockade, to angiotensin converting enzyme inhibition alone. By inhibiting neprilysin, which normally breaks down NPs, LCZ696 likely acts by activating PKG^{5,6}. Interestingly, other PKGI activating drugs, such as NPs, guanylate cyclase activators, and phosphodiesterase inhibitors, have had less clinical success in treating chronic heart failure (reviewed in 5). One suggested reason for these failures may be that in the setting of HF, maladaptive changes within cardiovascular tissue inhibit the ability of upstream signals to activate PKGI⁵. Therefore, targeting effectors downstream of PKGI might serve as a novel therapeutic strategy to circumvent these limitations of upstream PKGI activators. Further, hypotension arising from PKGI-induced vasodilation has proven a major limitation of PKGI-activating drugs in HF⁵. Focusing therefore on myocardial, rather than vascular, downstream substrates of PKGI α has the potential to identify therapeutic targets which might selectively inhibit cardiac remodeling yet avoid excess hypotension.

Importantly, small molecule MLK3 inhibitors themselves remain under investigation for the treatment of neurological conditions³⁶. Since our cell culture and *in vivo* data demonstrate that MLK3 normally attenuates pathologic remodeling, our findings suggest the possibility of undesired cardiac toxicities with MLK3 inhibition. Finally, we interpret our findings to suggest that augmenting, rather than inhibiting MLK3 activity or expression might prove to be a useful clinical strategy for the treatment of HF.

4.6 Significance of MLK3 as a PKGI α LZ-dependent substrate.

In addition to identifying MLK3 as a novel anti-remodeling protein, this study supports the more general hypothesis that exploring PKGI α LZ interacting proteins can reveal novel mechanisms governing cardiac hypertrophy, remodeling, and dysfunction. Prior studies in vascular biology have revealed a critical role of the LZ domain in mediating PKGI α interactions with vasodilating effector proteins. However, the role of the PKGI α LZ domain in cardiac remodeling has been investigated only more recently. In mice harboring discrete mutations of the PKGI α LZ domain, which disrupt LZ-dependent interactions, TAC induces accelerated LV contractile dysfunction and hypertrophy, leading to increased heart failure mortality¹¹. Further, mutation of the LZ domain reduced the anti-remodeling efficacy of PDE5 inhibition with sildenafil, supporting the mechanistic importance of PKG and LZ signaling in transmitting the anti-remodeling effect of cGMP. These published findings support a critical role for the LZ domain, and thus for LZ-dependent substrates, in inhibiting pressure overload-induced remodeling. However, the specific LZ substrates which inhibit remodeling had not been explored fully. Recently, a proteomic screen for myocardial LZ-binding proteins revealed cardiac myosin binding protein-C as a novel PKGI α binding protein and substrate⁸. However, while cMyBP-C represents a novel PKGI α substrate expressed selectively in the CM, its role in inhibiting cardiac remodeling had been established previously³⁷. Our identification of MLK3 as binding to the PKGI α LZ domain is of interest since MLK3 has not previously been implicated in cardiac biology or in cardiac remodeling. We therefore interpret these current findings to provide further evidence of a critical role of PKGI α LZ-dependent interactions in attenuating the pathologic cardiac remodeling

response. Identifying PKGI α LZ interacting proteins in the heart may reveal novel therapeutic targets for the treatment or prevention of heart failure.

4.7 Limitations.

Our study has several limitations. Most importantly, we obtained our *in vivo* data in mice with whole body, as opposed to tissue specific, MLK3 deletion. We therefore acknowledge that while our findings support a critical role of MLK3 in preserving heart function after pressure overload, they do not identify the specific cell type(s) mediating this effect. Animal models of tissue and temporal-specific disruption of MLK3 will be required to delineate the cell-specific effects of MLK3 in cardiovascular physiology and pathophysiology. Additionally, we acknowledge that additional and currently unknown downstream myocardial PKGI α anti-remodeling substrates may exist, but were not the focus of the present study.

We acknowledge as well that our human heart sample experiments were limited by relatively small numbers, thus reducing the statistical power of the experiments.

4.8 Conclusions.

In summary, we have identified MLK3 as a novel PKGI α substrate and LZ binding protein, which is expressed in the human heart, increases in expression in humans with HF, promotes JNK activation in the CM, and inhibits CM hypertrophy and cardiac remodeling *in vivo*. These findings identify MLK3 as a potential therapeutic target to inhibit cardiac remodeling, and support that PKGI α LZ dependent substrates function as anti-remodeling effectors.

References.

1. Lloyd-Jones D, Adams R, Carnethon M et al. Heart disease and stroke statistics--2009 update: a report from the American Heart Association Statistics Committee and Stroke Statistics Subcommittee. *Circulation*. 2009;119(3):480-6.
2. Jessup M, Brodena S. Medical Progress: Heart Failure. *N Engl J Med*. 2003;348:2007-14.
3. Molkentin J, Heineke J. Regulation of cardiac hypertrophy by intracellular signalling pathways. *Nature Rev Mol Cell Biol*. 2006;7:589-600.
4. Berenji K, Drazner MH, Rothermel BA, Hill JA. Does load-induced ventricular hypertrophy progress to systolic heart failure? *Am J Physiol Heart Circ Physiol*. 2005;289:H8-H16.
5. Kong Q, Blanton RM. Protein kinase G I and heart failure: Shifting focus from vascular unloading to direct myocardial antiremodeling effects. *Circ Heart Fail*. 2013;6:1268-83.
6. McMurray JJ, Packer M, Desai AS et al. Angiotensin-neprilysin inhibition versus enalapril in heart failure. *N Engl J Med*. 2014;371(11):993-1004.
7. Dupont JJ, McCurley A, Davel AP, McCarthy J, Bender SB, Hong K, Yang Y, Yoo JK, Aronovitz M, Baur WE, Christou DD, Hill MA, Jaffe IZ. Vascular mineralocorticoid receptor regulates microRNA-155 to promote vasoconstriction and rising blood pressure with aging. *JCI Insight*. 2016;1:e88942.
8. Thoonen R, Giovanni S, Govindan S et al. Molecular Screen Identifies Cardiac Myosin-Binding Protein-C as a Protein Kinase G-Ialpha Substrate. *Circ Heart Fail*. 2015;8(6):1115-22.
9. Surks HK, Mochizuki N, Kasai Y, Georgescu SP, Tang KM, Ito M, Lincoln TM, Mendelsohn ME. Regulation of myosin phosphatase by a specific interaction with cGMP- dependent protein kinase Ialpha. *Science*. 1999;286(5444):1583-7.
10. Surks HK, Mendelsohn ME. Dimerization of cGMP-dependent protein kinase Ialpha and the myosin-binding subunit of myosin phosphatase: role of leucine zipper domains. *Cell Signal*. 2003;15:937-44.
11. Blanton RM, Takimoto E, Lane AM, Aronovitz M, Piotrowski R, Karas RH, Kass DA, Mendelsohn ME. Protein kinase g α inhibits pressure overload-induced cardiac remodeling and is required for the cardioprotective effect of sildenafil in vivo. *J Am Heart Assoc*. 2012;1:e003731.
12. Tachibana H, Perrino C, Takaoka H, Davis RJ, Prasad SVN, Rockman HA. JNK1 is required to preserve cardiac function in the early response to pressure overload. *Biochem and Biophys Res Comm*. 2006;343:1060-1066.
13. Liang Q, Bueno OF, Wilkins BJ, Kuan C, Xia Y, Molkentin JD. C-Jun N terminal kinases (JNK) antagonize cardiac growth through cross-talk with calcineurin-NFAT signaling. *EMBO J*. 2003;22:5079-5089.
14. Maillet M, Lynch JM, Sanna B, York AJ, Zheng Y, Molkentin JD. Cdc42 is an antihypertrophic molecular switch in the mouse heart. *J Clin Invest*. 2009;119:3079-3088.
15. Liu W, Zi M, Chi H, Jin J, Prehar S, Neyses L, Cartwright EJ, Flavell RA, Davis RJ, Wang X. Deprivation of MKK7 in cardiomyocytes provokes heart failure in mice when exposed to pressure overload. *J Mol Cel Cardiol*. 2011;50:702-711.

16. Liu W, Zi M, Jin J, Prehar S, Oceandy D, Kimura TE, Lei M, Neyses L, Weston AH, Cartwright EJ, Wang X. Cardiac-specific deletion of MKK4 reveals its role in pathologic hypertrophic remodeling but not in physiological cardiac growth. *Circ Res*. 2009;104:905-914.
17. Sadoshima J, Montagne O, Wang Q, Yang G, Warden J, Liu J, Takagi G, Karoor V, Hong C, Johnson GL, Vatner DE, Vatner SF. The MEKK1-JNK pathway plays a protective role in pressure overload but does not mediate cardiac hypertrophy. *J Clin Invest*. 2002;110:271-279.
18. Rana A, Gallo K, Godowski P et al. The mixed lineage kinase SPRK phosphorylates and activates the stress-activated protein kinase activator, SEK-1. *J Biol Chem*. 1996;271(32):19025-8.
19. Du Y, Bock BC, Schachter KA, Chao M, Gallo KA. Cdc42 induces activation loop phosphorylation and membrane targeting of mixed lineage kinase 3. *J Biol Chem*. 2005;280(52):42984-93.
20. Kato M, Blanton R, Wang GR, Judson TJ, Abe Y, Myoishi M, Karas RH, Mendelsohn ME. Direct binding and regulation of RhoA by cyclic GMP-dependent protein kinase I α . *J Biol Chem*. 2012; 287:41342-41351. PMID: PMC3510832
21. Blom N, Sicheritz-Ponten T, Gupta R, Gammeltoft S, Brunak S. Prediction of post-translational glycosylation and phosphorylation of proteins from the amino acid sequence. *Proteomics*. 2004;4(6):1633-49.
22. O'Connell TD, Rodrigo MC, Simpson PC. Isolation and culture of adult mouse cardiac myocytes. *Methods Mol Biol*. 2007;357:271-96.
23. Lee DI, Zhu G, Sasaki T et al. Phosphodiesterase 9A controls nitric-oxide-independent cGMP and hypertrophic heart disease. *Nature*. 2015;519(7544):472-6.
24. Branco D, Ventura JJ, Jaeschke A, Doran B, Flavell RA, Davis RJ. Role of MLK3 in the regulation of mitogen-activated protein kinase signaling cascades. *Mol Cell Biol*. 2005;25(9):3670-81.
25. Rockman HA, Ross RS, Harris AN et al. Segregation of atrial-specific and inducible expression of an atrial natriuretic factor transgene in an in vivo murine model of cardiac hypertrophy. *Proc Natl Acad Sci U S A*. 1991;88(18):8277-81.
26. Vandewijngaert S, Pokreisz P, Hermans H, Gillijns H, Pellens M, Bax NA, Coppiello G, Oosterlinck W, Balogh A, Papp Z, Bouten CV, Bartunek J, D'hooge J, Luttun A, Verbeken E, Herregods MC, Herijgers P, Bloch KD, Janssens S. Increased cardiac myocyte PDE5 levels in human and murine pressure overload hypertrophy contribute to adverse LV remodeling. *PLoS One*. 2013;8(3): e58841. doi: 10.1371/journal.pone.0058841
27. Leung IW, Lassam N. The kinase activation loop is the key to mixed lineage kinase-3 activation via both autophosphorylation and hematopoietic progenitor kinase 1 phosphorylation. *J Biol Chem*. 2001;276(3):1961-7.
28. Das A, Smolenski A, Lohmann SM, Kukreja RC. Cyclic GMP-dependent protein kinase I α attenuates necrosis and apoptosis following ischemia/reoxygenation in adult cardiomyocyte. *J Biol Chem*. 2006;281(50):38644-52.
29. Goodfellow VS, Loweth CJ, Ravula SB et al. Discovery, synthesis, and characterization of an orally bioavailable, brain penetrant inhibitor of mixed lineage kinase 3. *J Med Chem*. 2013;56(20):8032-48.

30. Son Y, Kim S, Chung HT, Pae HO. Reactive oxygen species in the activation of MAP kinases. *Methods Enzymol.* 2013;528:27-48.
31. Tang M, Wang G, Lu P, et al. Regulator of G-protein signaling-2 mediates vascular smooth muscle relaxation and blood pressure. *Nat Med.* 2003;9:1506-12.
32. Wang Y, El-Zaru MR, Surks HK, Mendelsohn ME. Formin homology domain protein (FHOD1) is a cyclic GMP-dependent protein kinase I-binding protein and substrate in vascular smooth muscle cells. *J Biol Chem.* 2004;279(23):24420-6.
33. Veselka J, Anavekar NS, Charron P. Hypertrophic obstructive cardiomyopathy. *Lancet.* 2016;S0140-6736(16)31321-6. doi: 10.1016/S0140-6736(16)31321-6. [Epub ahead of print]
34. Wooten EC, Hebl VB, Wolf MJ, Greytak SR, Orr NM, Draper I, Calvino JE, Kapur NK, Maron MS, Kullo IJ, Ommen SR, Bos JM, Ackerman MJ, Huggins GS. Formin homology 2 domain containing 3 variants associated with hypertrophic cardiomyopathy. *Circ Cardiovasc Genet.* 2013;6(1):10-8.
35. Choukroun G, Hajjar R, Kyriakis JM, Bonventre JV, Rosenzweig A, Force T. Role of the stress-activated protein kinases in endothelin-induced cardiomyocyte hypertrophy. *J Clin Invest.* 1998;102(7):1311-20.
36. Marker DF, Tremblay ME, Puccini JM et al. The new small-molecule mixed-lineage kinase 3 inhibitor URMC-099 is neuroprotective and anti-inflammatory in models of human immunodeficiency virus-associated neurocognitive disorders. *J Neurosci.* 2013;33(24):9998-10010.
37. Sadayappan S, Osinska H, Klevitsky R, Lorenz JN, Sargent M, Molkenin JD, Seidman CE, Seidman JG, Robbins J. Cardiac myosin binding protein c phosphorylation is cardioprotective. *Proc Natl Acad Sci.* 2006;103:16918-16923.